Research article

Journal of MASS SPECTROMETRY

Received: 14 December 2014 Revised: 14 March 2015 Accepted: 22 April 2015 Published online in Wiley Online Library

(wileyonlinelibrary.com) DOI 10.1002/jms.3607

Identification of position isomers by energy-resolved mass spectrometry

Sunil Paul M. Menachery,[a] Olivier Laprévote,[b] Thao P. Nguyen,[c] Usha K. Aravind,[d] Pramod Gopinathan[e] and Charuvila T. Aravindakumar[a,f]*

This study reports an energy-resolved mass spectrometric (ERMS) strategy for the characterization of position isomers derived from the reaction of hydroxyl radicals (•OH) with diphenhydramine (DPH) that are usually hard to differentiate by other methods. The isomer analogues formed by •OH attack on the side chain of DPH are identified with the help of a specific fragment ion peak (*m/z* 88) in the collision-induced dissociation (CID) spectrum of the protonated molecule. In the negative ion mode, the breakdown curves of the deprotonated molecules show an order of stability (supported by density functional theory (DFT) calculations) *ortho* > *meta* > *para* of the positional isomers formed by the hydroxylation of the aromatic ring. The gas phase stability of the deprotonated molecules $[M-H]^-$ towards the benzylic cleavage depends mainly on the formation of intramolecular hydrogen bonds and of the mesomeric effect of the phenol hydroxyl. The $[M-H]^-$ molecules of ortho and meta isomers result a peak at *m/z* 183 with notably different intensities because of the presence/absence of an intramolecular hydrogen bonding between the OH group and C9 protons. The ERMS approach discussed in this report might be an effective replacement for the conventional methods that requires very costly and time-consuming separation/purification methods along with the use of multi-spectroscopic methods. Copyright © 2015 John Wiley & Sons, Ltd.

Additional supporting information may be found in the online version of this article at the publisher's web site.

Keywords: position isomerism; energy-resolved mass spectrometry; hydroxyl radicals; collision-induced dissociation; mesomeric effect

Introduction

The crucial role of hydroxyl radicals (•OH) in the oxidative destruction of environmental pollutants in Advanced Oxidation Processes (AOPs) and in many biological processes including DNA damage, mutation and ageing is well established.[1–8] The non position-selective reaction of •OH with aromatic compounds generates isomeric hydroxylated compounds in various chemical processes.[6,9,10] The exact structural assignments of the transient absorption spectra obtained by pulse radiolysis experiments (a widely used technique to probe the spectroscopic details of the transient intermediate species) are consequently very difficult, and hence many authors interpret the experimental spectra in to a cumulative effect of undistinguishable OH adducts.[6,10–13] An important challenge in analytical chemistry over the past few decades was therefore the development of suitable techniques for the rapid characterization of these isomers. Nuclear magnetic resonance (NMR) spectroscopy is an undisputed tool for the chemical characterization of any kind of organic molecules. However, requirement of relatively large sample amounts, high cost of deuterated solvents and complicated (and costly) pre-separation/purification steps are the major drawback of this technique.[14] Another possibility is the use of authentic standards that are relatively costly and unavailable in many cases. The utilization of tandem mass spectrometry alone is exceedingly difficult in this context because of the close structural similarities of hydroxylated isomers. In a previous report, Fu *et al*. suggested that the exact structural assignment of individual isomers is very challenging because of the close resemblances in the collision-induced dissociation (CID) spectra (commonly referred as MS/MS spectra) even though the liquid chromatography (LC) system can separate each of them.[15]

A possible alternative to gain the structural characteristics of these isomers is the investigation of the fragmentation of their gas phase ions using energy-resolved mass spectrometry (ERMS). The technique involves the collisional activation of the gas phase ions either at the interface of an electrospray ionization source or by means of an inert collision gas in tandem mass spectrometry.[16,17] By using the low-energy collisional activation and tandem mass spectrometry, one can control the amount of energy transferred in to an ion by varying the collision energy (CE) and

* *Correspondence to: Charuvila T. Aravindakumar, Inter University Instrumentation Centre (IUIC), Mahatma Gandhi University, Priyadarsini Hills, Kottayam, Kerala. India. E-mail: cta@mgu.ac.in*

a *School of Environmental Sciences, Mahatma Gandhi University, Priyadarsini Hills, Kottayam, Kerala, India*

b *Laboratory of Analytical Chemistry and Experimental Toxicology, University Paris Descartes, Paris, France*

c *Department of Chemistry, Pohang University of Science and Technology (POSTECH), Pohang 790-784, Republic of Korea*

d *Advanced Centre of Environmental Studies and Sustainable Development (ACESSD), Mahatma Gandhi University, Priyadarsini Hills, Kottayam, Kerala, India*

e *Department of Chemistry, N.S.S. Hindu College, Changanachery, Kerala, India*

f *Inter University Instrumentation Centre (IUIC), Mahatma Gandhi University, Priyadarsini Hills, Kottayam, Kerala, India*

Journal of MASS SPECTROMETRY

accordingly the fragmentation rate. The compound specific ERMS curves are therefore exploited by many authors for the characterization of position and stereo isomers and even for conformational analysis.[16–19]

In this report, we present an ERMS-based strategy for the rapid characterization of position isomers derived from the reaction of $^{\bullet}$OH with diphenhydramine (DPH), a first-generation antihistamine and a potential candidate from the group of so-called 'emerging organic contaminants'. Destruction of this compound by various AOPs is thoroughly experimented.[9,20] Very recently, Feng *et al.* reported that the reaction of $^{\bullet}$OH on DPH yields different isomeric hydroxylated compounds.[9] The authors were however unable to characterize the individual isomers because of the lack of significant differences in the MS/MS spectra. Testa *et al.* suggested that the pharmacological activities and the affinity for specific targets were retained in the case of hydroxylated metabolites.[21] Characterizations of these isomeric compounds are thus very interesting and highly important for the evaluation of the pharmacological (and hence toxicological) status of these reactions. Further, the minute structural details of these kinds are very necessary to obtain an in-depth understanding of the transformation mechanism of DPH which is utmost important in biological and environmental systems. To the best of our knowledge, this is the first report on the application of ERMS for the characterization of position isomers derived from the reaction of $^{\bullet}$OH with any organic molecule of biological and environmental importance, though a number of ERMS-based isomeric characterizations were experimented with authentic standards.[10,16,17,19,22]

Materials and methods

Diphenhydramine (CAS No. 58-73-1) was purchased from Sigma Aldrich and was used without further purification. All other reagents used in the present study were in the highest available purities. The various hydroxylated analogues of DPH were analysed by ultra performance liquid chromatography (UPLC) coupled with a quadrupole-time-of-flight (Q-TOF) high resolution mass spectrometer (Xevo G2, Waters, USA). The samples were ionized by electrospray ionization (ESI) after separating on a BEH C18 column (100 mm × 2.1 mm × 1.7 μm, Waters). An elution gradient of methanol and water (both having 1 mM ammonium acetate) at a flow rate of 0.25 ml min^{-1} was used as the mobile phase. The mass spectra were recorded in both positive and negative ionization modes in *m/z* ranges of 50–600 Th. The CID spectra were recorded by fragmenting the selected precursor ions by collision with high purity argon gas. For obtaining mass accuracy in high resolution mass spectra, leucine enkephalin ($[M+H]^+$: 556.2771; $[M-H]^-$: 554.2615) was used as a reference standard.[23] The stability of different isomeric hydroxylated DPH analogues, identified by the high resolution mass spectrometry, was further evaluated by ERMS analysis. The ERMS curves were determined by recording the CID spectrum of individual compounds using a series of collision energies (CE) starting from 6 eV and increased until the precursor ions no longer exist. The structures of tested subjects were fully relaxed without geometry constraint using density functional theory (DFT) calculations with hybrid B3LYP functional using basis set 6-31G, 6-31G(d,p) and polarized basis set 6-31G+, 6-31G+(d). In addition B3PW91 method with basis set 6-31G+ was used, and a comparative study on the effect of basis sets on the calculated structures was performed. All the calculations were carried out using Gaussian 09 W in order to predict the relative stability of individual isomers.[24]

Results and discussion

Photo-irradiation experiments of the aqueous solution of DPH in the presence of H_2O_2 were performed on a medium pressure mercury lamp (254 nm)-based photo-reactor. The interaction of UV radiation with H_2O_2 is reported to produce $^{\bullet}$OH in the medium according to reaction 1.[11]

$$H_2O_2 + h\nu \rightarrow 2^{\bullet}OH \quad (1)$$

Analysis of hydroxylated products by mass spectrometry

The samples resulting from the photo-irradiation experiments were subjected to HRMS analysis to elucidate the identity of the major transformation products formed during the reaction. Total ion chromatogram (TIC) in the positive ionization mode as shown in Fig. S1 shows four reasonably resolved peaks at RT 4.6 (**A**), 4.7 (**B**), 4.9 (**C**) and 5.2 min (**D**) corresponding to a mass-to-charge ratio (*m/z*) of 272 (obs. 272.1646; calcd. for $C_{17}H_{22}NO_2$ 272.1645). The comparison of the accurate mass and the elemental composition of these peaks with that of the parent molecule (obs. 256.1697; calcd. for $C_{17}H_{22}NO$ 256.1701) suggested that the difference in the *m/z* value is likely because of the hydroxylation of the parent compound.

CID experiments in positive ionization mode

Further, structural features are gained by performing CID experiments of the respective precursor ions $[M+H]^+$. The corresponding MS/MS spectra are shown in Fig. 1. The protonated molecules of **A**, **B** and **C** at *m/z* 272 led to an abundant fragment at *m/z* 183 (obs. 183.0814; calcd. for $C_{13}H_{11}O$ 183.0810). This *m/z* value is around 16 Da higher than 167 (obs. 167.0857; calcd. for $C_{13}H_{11}$ 167.0861), which is the major fragment observed in the MS/MS spectrum of protonated DPH. On the basis of the above observations, it is suggested that the mass difference of 16 Da is because of the hydroxylation of the aromatic part of DPH.

Conversely, the MS/MS spectrum of **D** exhibits an intense fragment at *m/z* 167. Because of the presence of a similar fragment in the MS/MS spectrum of the parent molecule (Fig. S2), it seems highly logical that the aromatic part of this hydroxylated derivative remained intact, the hydroxyl group being located on the side chain. The hydrogen abstraction reaction of $^{\bullet}$OH from one of the methyl hydrogen atoms of DPH followed by further hydroxylation is a probable explanation for the formation of this product. A similar product was also observed by Feng *et al.* during their end-product studies.[9] To explain the identity of this compound, the authors propose a C_{10}-hydroxyl substituted DPH analogue with the help of limited MS/MS studies. However, the assignment of an exact structure for this spectrum in the case of compounds like DPH seems to be very difficult because of the availability of more than one hydrogen atoms (one at C_7, two at C_9 and C_{10} and three at C_{12} and C_{13}, Scheme 1) which could be the target of $^{\bullet}$OH attack.

The small, however potentially important, fragment at *m/z* 88 (obs. 88.0767; calcd. for $C_4H_{10}NO$ 88.0762) in the MS/MS spectrum of D was not observed in the case of other precursor ions of **A–C** (Fig. 2). This fragment ion allows the assignment of compound D as either the C_{10} (an identical structure proposed by Feng *et al.*)[9] or C_{12}/C_{13} hydroxylated derivative of DPH. This assignment is based

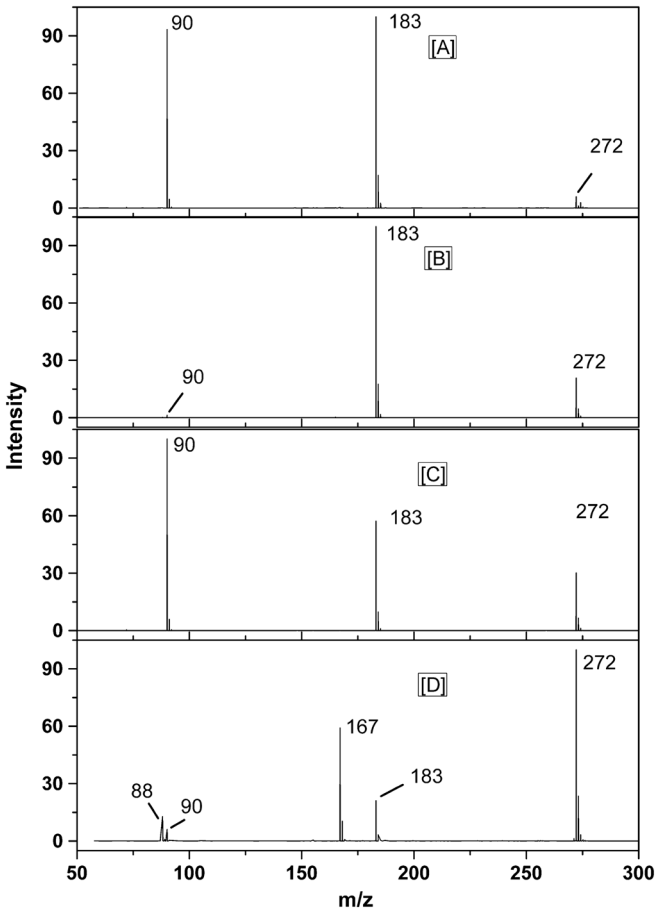

Figure 1. The CID spectra of the protonated ions of A–D. Collision energy: 10 eV.

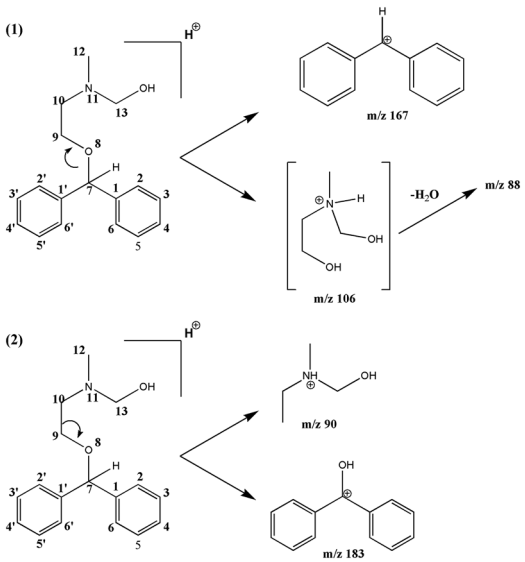

Scheme 1. Proposed fragmentation pathways of the (M + H) + ion (*m/z* 272) of D leading to the formation of fragment ions at *m/z* 167, 88 (1), 183 and 90 (2).

on the observed instability of the *N*-hydroxymethyl intermediate which leads to a diphenylmethylium ion (*m/z* 167) by benzylic dissociation of the precursor ion $[\mathbf{D}+\mathrm{H}]^+$ (Scheme 1). The loss of a

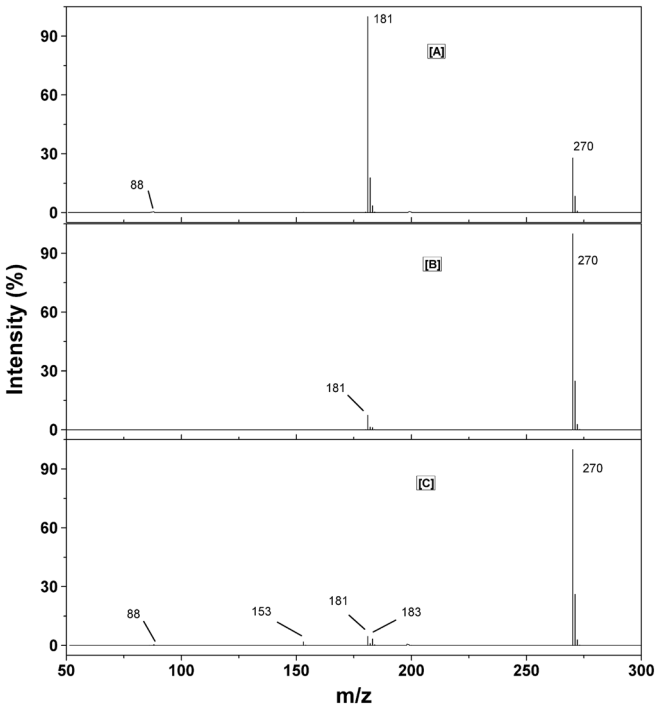

Figure 2. CID spectra of the deprotonated molecules of A–C (*m/z* 270). Collision energy: 10 eV.

molecule of water from the complementary fragment ion at *m/z* 106 is very likely at the origin of the *m/z* 88 ion signal (Scheme 1). Reports on the benzylic dissociation in the case of diarylpyrimidines, benzyl esters and thioethers are available in the literature.[25] The MS/MS spectrum reported by Feng *et al.*[9] however lacks the fragment ion peaks at *m/z* 88, 90 and 167. It is thus reasonable to rule out the C_{10} hydroxylated analogue of DPH from the present case. The possibility of $^{\bullet}$OH attack on the nitrogen atom of DPH seems very unlikely because of the lack of stabilization of resulting nitrogen-centred radical cation. The above stated reasons allow us to attribute a C_{12}/C_{13} hydroxylated derivative of DPH for isomer **D**. Relatively less intense fragments at *m/z* 90 (obs. 90.0919; calcd. for $C_4H_{12}NO$ 90.0919) and 183 (obs. 183.0808; calcd. for $C_{13}H_{11}O$ 183.0811) were also observed in this spectrum (Fig. 1D). The identity of these fragment ions in the case of $[\mathbf{D}+\mathrm{H}]^+$ is rationalized by the dissociation of oxygen (O_8)–carbon (C_9) bond as shown in Scheme 1.

On the other hand, three distinguished sites namely *ortho* (2, 2′, 6, 6′), *meta* (3, 3′, 5, 5′) and *para* (4, 4′) are available for $^{\bullet}$OH attack on the aromatic part of DPH (Scheme 1). The exact assignments of the individual isomers (A–C) are very difficult at this stage because of the close structural features and significant similarities in the MS/MS spectra. However, identification of the corresponding isomeric hydroxylated products of DPH, which might include *ortho*, *meta* and *para* derivatives, is utmost important for evaluating the pharmacological activities of the metabolites/transformation products of compounds like DPH.

CID experiments in negative ionization mode

In order to simplify the interpretation, the CID spectra corresponding to deprotonated **A–C** were recorded in the negative ionization mode. It is noteworthy to mention the absence of peak **D** in the case of the negative ionization mode (Fig. S1). A likely reason for

Journal of MASS SPECTROMETRY

the absence of this peak is the lack of ionization of the corresponding product. It can be attributed to a lower gas-phase acidity of the alcohol function with regards to the phenol group. The influence of the hydroxylation site (such as *ortho*, *meta* and *para*) on the gas-phase stability of the protonated molecules of **A–C** is however much less significant because the OH group is far away from the protonation site (very likely the tertiary amino group). By contrast, the stability of the deprotonated molecules of **A–C** (obs. 270.1494; calcd. for $C_{17}H_{20}NO_2$ 270.1494) is expected to be drastically affected by the position of the hydroxyl group because of the involvement of the negative charge in the aromatic system and of the expected mesomeric effects on the benzylic bond dissociation. Consequently, the ease in fragmentation of these ions is likely different for **A–C**. In this context, it was assumed that the differences in the MS/MS spectra and ERMS curves of different ion peaks could offer valuable information about the exact position of the OH group.

The MS/MS spectra of the deprotonated molecules of **A–C** are largely different (Fig. 2). The precursor ions $[\mathbf{A}-H]^-$ and $[\mathbf{B}-H]^-$ led to an identical fragment at *m/z* 181 (obs. 181.0653; calcd. for $C_{13}H_9O$ 181.0653) but with very different intensities. Comparison of the CID spectra of the $[\mathbf{B}-H]^-$ and $[\mathbf{C}-H]^-$ precursor ions at *m/z* 270 showed an additional ion peak at *m/z* 183 (obs. 183.0804; calcd. for $C_{13}H_{11}O$ 183.0811) for the compound **C** with an intensity similar to the *m/z* 181 ion. A small, however potentially important, peak at *m/z* 88 (obs. 88.0756; calcd. for $C_4H_{10}NO$ 88.0762) was observed in the case of $[\mathbf{A}-H]^-$ and $[\mathbf{C}-H]^-$ whereas this fragment was not observed in the CID spectrum of $[\mathbf{B}-H]^-$. Additionally, a peak at *m/z* 153 (obs. 153.0700; calcd. for $C_{12}H_9$ 153.0704) is visible in the case of the **C** isomer. An extremely small peak at *m/z* 199 (obs. 199.0755; calcd. for $C_{13}H_{11}O_2$ 199.0759) is also observed in the case of **A** and **C**. Further, the intensity of the precursor ion $[\mathbf{A}-H]^-$ was less than 30% at a CE of 10 eV whereas the other two precursor ions formed from **B** and **C** showed a much higher gas-phase stability under the same CE conditions.

Theoretical calculations

Theoretical calculations of gas phase deprotonated ions using DFT method have been mainly carried out to find out the relative stabilities of individual isomers. The two different DFT methods used in this study showed very similar result in predicting the stability of each ion. The optimized geometries of gas phase deprotonated ions of *ortho*, *meta* and *para* are shown in Fig. 3. Application of polarized basis sets showed a slight decrease in the molecular energy difference among three isomers compared to 6-31G(d,p) and 6-31G basis sets. However, all of the methods showed the same trend and indicated that there is a big gap in energy between *meta* and *ortho* isomer predicting the stability in *ortho* structure. The results clearly showed that the gas phase ion of *ortho* analogue has the lowest energy and is therefore the most stable. The energy difference (B3LYP/6-31G+(d)) between *ortho* to *meta* and *meta* to *para* (least stable) were 3.16 and 1.93 kcal mol^{-1}, respectively. More specific results are shown in Table S1.

It is clearly visible from the optimized structure of *ortho* isomer (Fig. 3) that the electronegative deprotonated phenol oxygen and the alkyl hydrogen atoms are very close to each other. The stabilization of gas phase ions by hydrogen bonding is reported in the case of a range of compounds including biomolecules.[16,26,27] In the case of *ortho* isomer, it is thus very logical to expect the formation of an intramolecular hydrogen bonding between the above specified atoms. A similar stabilization in the case of *meta* and *pare* analogues is however very unlikely because the phenol oxygen is geometrically very far from the alkyl hydrogen atoms. On the basis of theoretical calculations, it is thus expected that the gas phase deprotonated ion of the *para* isomer induces higher fragmentation rates.

ERMS analysis

To predict the stability of various deprotonated ions, ERMS studies were performed on a range of CE. The results are shown in Fig. 4. The relative ion current corresponding to the individual ions was calculated using the following equation, where Ci and Cp stand

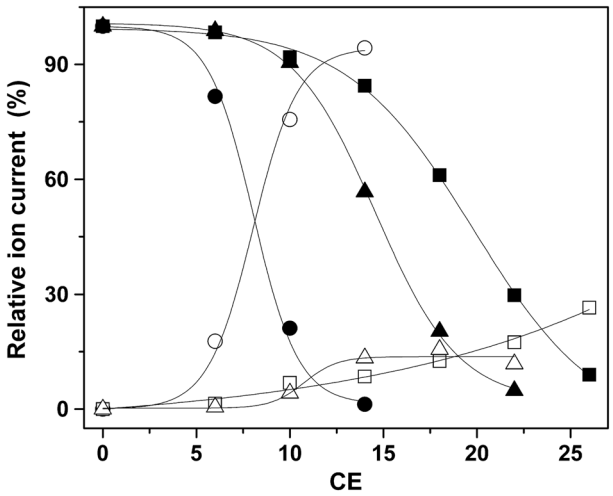

Figure 4. Plot of relative ion current *versus* collision energy corresponding to *m/z* 270 (A (•), B (▪) and (▲) C) and *m/z* 181 (A (o), B (□) and (◊) C).

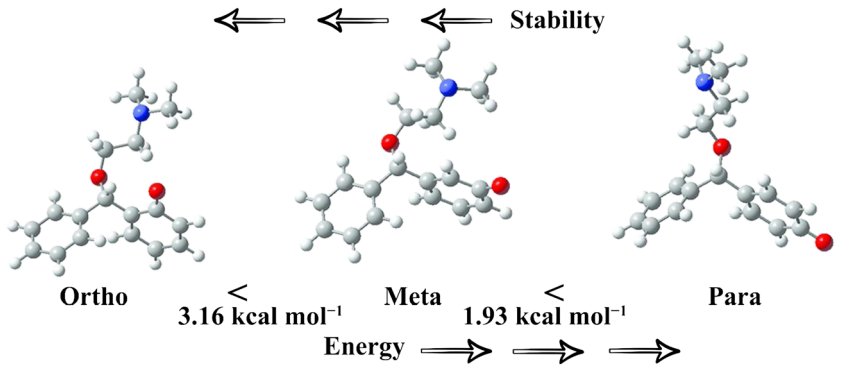

Figure 3. Optimized structure of the deprotonated gas phase ions of A–C (basis set B3LYP/6-31G+(d)).

for the observed ion current of a specific product ion as well as the parent ion, respectively.[28]

$$^{rel}C = 100 \times \left(Ci / \left(Cp + \sum Ci \right) \right) \quad (2)$$

The ERMS curves of the deprotonated molecules displayed a 50% dissociation rate of the $[\mathbf{A} - H]^-$ ion at a CE of near 8.0 eV with a fast increase of the intensity of the fragment ion at *m/z* 181 (Fig. 4). By comparison, $[\mathbf{B} - H]^-$ and $[\mathbf{C} - H]^-$ were much more stable showing a 50% dissociation rate at 19.5 and 14.5 eV, respectively. Further, the enhancement of the *m/z* 181 fragment intensities was relatively slow in the case of the deprotonated **B** and **C** molecules suggesting a much higher stability of these ions toward this fragmentation pathway.

The presence of hydroxyl groups at the *ortho* and *para* positions is an important factor that enhances the benzylic dissociation responsible for the formation of the dimethylamino ethanolate anion (*m/z* 88) along with the complementary *ortho*/*para* quinone methide ion as depicted in Scheme 2. The cleavage of the benzylic carbon–oxygen bond leads directly to the *m/z* 88 fragment ion or, *via* a proton transfer within an intermediate ion-neutral complex, to the fragment at *m/z* 181. The involvement of phenol oxygen atom in the intramolecular hydrogen bonding, that reduces electron density, however restricts this mesomeric enhancement in the case of *ortho* isomer. Furthermore, the fragmentation of the benzylic bond is expected to be less effective in the case of the *meta* analogue because of the lack of any mesomeric enhancement. These effects should reduce the fragmentation rate of the deprotonated *ortho* and *meta* isomer and increase its gas-phase stability. Because the ERMS analysis reveals that the stability of the deprotonated molecules are in the order **B** > **C** > **A** (Fig. 4), we assigned the *ortho* structure, which is predicted as the most stable one by theoretical calculations, to the compound **B**. The two other structures, i.e. *meta* and *para*, remained to be attributed to the compounds **A** and **C**. The deprotonated ion of compound **A** was clearly the less stable one and was then assigned the structure *para*. Indeed the position of the phenoxy group does not allow any intramolecular hydrogen bonding between the negative charge and the rest of the structure. As a consequence, the compound **C** was identified as the *meta* isomer.

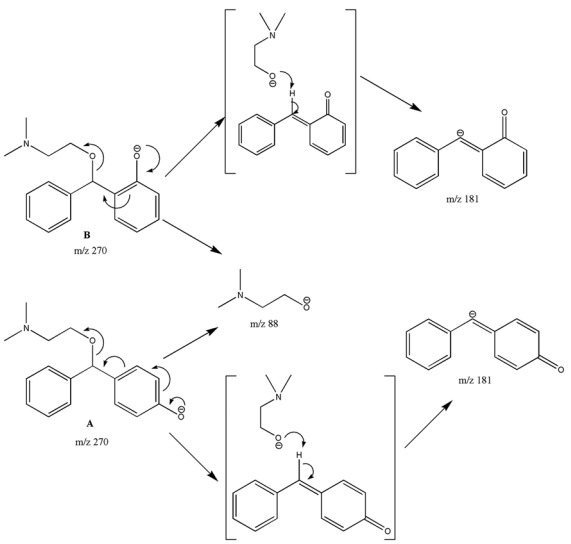

Scheme 2. Proposed fragmentation pathways of *m/z* 270 ion derived from A and B.

Further, the fragment at *m/z* 183 which was observed in the case of **C** and which led to a very weak signal for **B** explicitly justifies the assessment of *ortho* and *meta* isomers in to **B** and **C**, respectively (Fig. 2). Formation of this fragment is indeed easily rationalized with the help of an intramolecular proton transfer followed by the release of a (dimethylamino)acetaldehyde moiety as depicted in Scheme 3.

The proposed mechanism corresponding to the formation of *m/z* 183 is very unlikely in the case of *para* analogue because of the large distance between the phenoxide group and the alkyl hydrogen atoms. The absence (or very negligible intensity) of this fragment in the MS/MS spectrum of the *para* isomer is hence unambiguously anticipated. It is noteworthy to specify that the small ion peaks at *m/z* 182 (obs. 182.0683) and 183 (obs. 183.0769) observed in the MS/MS spectrum of A (Fig. 2) are mainly because of the contribution from ^{13}C isotope of fragment ion peak at *m/z* 181, and then significantly differ from the *m/z* 183 fragment ion (obs. 183.0804) formed from deprotonated **B** and **C**. The intramolecular hydrogen bonding involved in the case of *ortho* analogue is expected to restrict the feasibility of this fragmentation pathway though phenoxide group is very near to the alkyl hydrogen atoms. Consequently, the intensity of the corresponding fragment at *m/z* 183 is very much weaker in the case of the $[\mathbf{B} - H]^-$ ion. The reasonable distance between the phenoxide group and alkyl hydrogen atoms and the lack of intramolecular hydrogen bonding result the most intense fragment peak corresponding to *m/z* 183, which is more or less equal to that of the fragment at *m/z* 181, in the case of *meta* isomer (Fig. 2).

Formation of remaining fragment ion such as *m/z* 153 and 199 is explained in Scheme 4. The small fragment at *m/z* 153, which is observed in the case of **C** (Fig. 2) as well as in the case of **A** and **B** at higher CE values of 22 and 18, respectively (Figure S3 and S4), is rationalized by a routine loss of CO (27.9949) from the fragment at *m/z* 181 and corresponds to a cyclopentadienyl-type

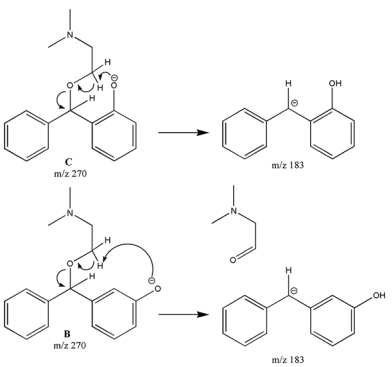

Scheme 3. Proposed fragmentation pathway leading to the formation of the fragment ion at *m/z* 183.

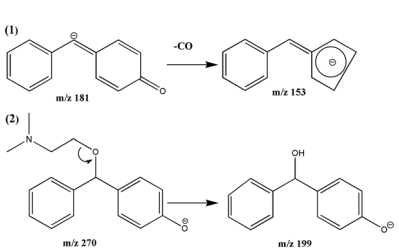

Scheme 4. Proposed fragmentation pathway leading to the formation of fragment ions at *m/z* 153 (1) and 199 (2).

Journal of MASS SPECTROMETRY

anion. The minute fragments observed at *m/z* 199 in the case of *para* and *meta* analogues are likely due to a similar dissociation of carbon–oxygen bond as explained in the case of protonated molecule of **D**. The proposed structure of fragment ions at *m/z* 153 and 199 is depicted in Scheme 4.

Conclusions

In conclusion, a very simple, rapid and cost-effective method, based on energy-resolved mass spectrometry, has been developed for the real-time characterization of position isomers (such as *ortho*, *meta* and *para*) derived from the reaction of hydroxyl radical with diphenhydramine. Because of the close structural similarities, the characterization of position isomers of these kind otherwise requires highly difficult and costly separation/purification procedures and the use of multi spectroscopic techniques such as nuclear magnetic resonance (NMR) and infrared (IR) spectroscopy. The present strategy does not necessitate any time consuming purification steps and use of any costly standards. It allows real-time characterization of the position isomers within a chromatographic run time of 6 min. In this context, the novel ERMS-based methodology demonstrated in the present study is extremely relevant. Further studies are however necessary for the development of a more generalized procedure applicable for more number of molecules which are currently in progress.

Acknowledgements

This work was performed under collaborative research scheme (Ref No. UGC-DAE-CSR-KC/CRS/09/RC02/1455) of UGC-DAE Consortium for Scientific Research, Kolkata Centre, Kolkata. The authors acknowledge Dr. Ji Hoon Shim, Department of Chemistry, Pohang University of Science and Technology (POSTECH), Republic of Korea, for the computational facility. CTA is thankful to DST (under PURSE and FIST scheme) and KSCSTE for financial support. GP is thankful to SB College, Changanasserry for research guideship.

References

[1] J. M. Poyatos, M. M. Muñio, M. C. Almecija, J. C. Torres, E. Hontoria, F. Osorio. Advanced oxidation processes for wastewater treatment: State of the art. *Water Air Soil Pollut.* **2010**, *205*, 187.
[2] S. Steenken. Purine bases, nucleosides, and nucleotides: Aqueous solution redox chemistry and transformation reactions of their radical cations and e- and OH adducts. *Chem. Rev.* **1989**, *89*, 503.
[3] J. Cadet, T. Douki, J.-L. Ravanat. Oxidatively generated base damage to cellular DNA. *Free Radic. Biol. Med.* **2010**, *49*, 9.
[4] C. Chatgilialoglu, M. D'Angelantonio, M. Guerra, P. Kaloudis, Q. G. Mulazzani. A Reevaluation of the ambident reactivity of the guanine moiety towards hydroxyl radicals. *Angew. Chem. Int. Ed.* **2009**, *48*, 2214.
[5] V. M. Manoj, C. T. Aravindakumar. Hydroxyl radical induced decomposition of S-nitrosoglutathione. *Chem. Commun.* **2000**, 2361.
[6] R. Sreekanth, K. P. Prasanthkumar, M. M. Sunil Paul, U. K. Aravind, C. T. Aravindakumar. Oxidation reactions of 1- and 2-Naphthols: An experimental and theoretical study. *J. Phys. Chem. A* **2013**.
[7] M. M. Sunil Paul, U. K. Aravind, G. Pramod, C. T. Aravindakumar. Oxidative degradation of fensulfothion by hydroxyl radical in aqueous medium. *Chemosphere* **2013**, *91*, 295.
[8] J. A. Theruvathu, C. T. Aravindakumar, R. Flyunt, J. von Sonntag, C. von Sonntag. Fenton chemistry of 1,3-Dimethyluracil. *J. Am. Chem. Soc.* **2001**, *123*, 9007.
[9] X. Feng, Z. Wang, Y. Chen, T. Tao, F. Wu, Y. Zuo. Effect of Fe(III)/Citrate concentrations and ratio on the photoproduction of hydroxyl radicals: Application on the degradation of diphenhydramine. *Ind. Eng. Chem. Res.* **2012**, *51*, 7007.
[10] R. Sreekanth, S. P. M. Menachery, U. K. Aravind, J.-L. Marignier, J. Belloni, C. T. Aravindakumar. Oxidation reactions of hydroxy naphthoquinones: Mechanistic investigation by LC-Q-TOF-MS analysis. *Int. J. Radiat. Biol.* **2014**, *90*, 495.
[11] G. V. Buxton, C. L. Greenstock, W. P. Helman, A. B. Ross. Critical review of rate constants for reactions of hydrated electrons, hydrogen atoms and hydroxyl radicals ([center-dot]OH/[center-dot]O[sup -] in aqueous solution. *J. Phys. Chem. Ref. Data* **1988**, *17*, 513.
[12] M. S. Kulkarni, P. Yadav, M. B. Shirdhonkar, B. S. M. Rao. Pulse radiolysis: Pune University LINAC facility. *Curr. Sci.* **2007**, *92*, 599.
[13] M. M. Sunil Paul, U. K. Aravind, G. Pramod, A. Saha, C. T. Aravindakumar. Hydroxyl radical induced oxidation of theophylline in water: A kinetic and mechanistic study. *Org. Biomol. Chem.* **2014**, *12*, 5611.
[14] C. Prakash, C. L. Shaffer, A. Nedderman. Analytical strategies for identifying drug metabolites. *Mass Spectrom. Rev.* **2007**, *26*, 340.
[15] S. Fu, D. Arráez-Román, J. A. Menéndez, A. Segura-Carretero, A. Fernández-Gutiérrez. Characterization of isomers of oleuropein aglycon in olive oils by rapid-resolution liquid chromatography coupled to electrospray time-of-flight and ion trap tandem mass spectrometry. *Rapid Commun. Mass Spectrom.* **2009**, *23*, 51.
[16] O. Laprévote, P. Ducrot, C. Thal, L. Serani, B. C. Das. Stereochemistry of electrosprayed Ions. Indoloquinolizidine derivatives. *J. Mass Spectrom.* **1996**, *31*, 1149.
[17] D. Lemaire, L. Serani, O. Laprévote, V. Ovcharenko, K. Pihlaja, G. Stájer. Energy-resolved electrospray mass spectrometry of diexo-norbornane and norbornene derivatives containing a fused, phenyl-substituted, 1,3-oxazine ring: Competitive retro-Diels-Alder fragmentation processes. *Eur. J. of Mass Spectrom.* **1999**, *5*, 253.
[18] A. F. Lehner, J. Horn, J. W. Flesher. Formation of radical cations in a model for the metabolism of aromatic hydrocarbons. *Biochem. Biophys. Res. Commun.* **2004**, *322*, 1018.
[19] A. B. Attygalle, J. Ruzicka, D. Varughese, J. B. Bialecki, S. Jafri. Low-energy collision-induced fragmentation of negative ions derived from ortho-, meta-, and para-hydroxyphenyl carbaldehydes, ketones, and related compounds. *J. Mass Spectrom.* **2007**, *42*, 1207.
[20] L. M. Pastrana-Martínez, J. L. Faria, J. M. Doña-Rodríguez, C. Fernández-Rodríguez, A. M. T. Silva. Degradation of diphenhydramine pharmaceutical in aqueous solutions by using two highly active TiO2 photocatalysts: Operating parameters and photocatalytic mechanism. *Appl. Catal. Environ.* **2012**, *113–114*, 221.
[21] B. Testa, A. Pedretti, G. Vistoli. Reactions and enzymes in the metabolism of drugs and other xenobiotics. *Drug Discov. Today* **2012**, *17*, 549.
[22] A. Attygalle, J. Ruzicka, D. Varughese, J. Sayed. An unprecedented ortho effect in mass spectrometric fragmentation of even-electron negative ions from hydroxyphenyl carbaldehydes and ketones. *Tetrahedron Lett.* **2006**, *47*, 4601.
[23] J. Sztaray, A. Memboeuf, L. Drahos, K. Vekey. Leucine enkephalin–a mass spectrometry standard. *Mass Spectrom. Rev.* **2011**, *30*, 298.
[24] M. J. Frisch, G. W. Trucks, H. B. Schlegel, G. E. Scuseria, M. A. Robb, J. R. Cheeseman, G. Scalmani, V. Barone, B. Mennucci, G. A. Petersson, H. Nakatsuji, M. Caricato, X. Li, H. P. Hratchian, A. F. Izmaylov, J. Bloino, G. Zheng, J. L. Sonnenberg, M. Hada, M. Ehara, K. Toyota, R. Fukuda, J. Hasegawa, M. Ishida, T. Nakajima, Y. Honda, O. Kitao, H. Nakai, T. Vreven, J. A. Montgomery Jr., J. E. Peralta, F. Ogliaro, M. J. Bearpark, J. Heyd, E. N. Brothers, K. N. Kudin, V. N. Staroverov, R. Kobayashi, J. Normand, K. Raghavachari, A. P. Rendell, J. C. Burant, S. S. Iyengar, J. Tomasi, M. Cossi, N. Rega, N. J. Millam, M. Klene, J. E. Knox, J. B. Cross, V. Bakken, C. Adamo, J. Jaramillo, R. Gomperts, R. E. Stratmann, O. Yazyev, A. J. Austin, R. Cammi, C. Pomelli, J. W. Ochterski, R. L. Martin, K. Morokuma, V. G. Zakrzewski, G. A. Voth, P. Salvador, J. J. Dannenberg, S. Dapprich, A. D. Daniels, Ö. Farkas, J. B. Foresman, J. V. Ortiz, J. Cioslowski, D. J. Fox. *Gaussian 09, Revision A.02*. Gaussian, Inc.: Wallingford, CT, USA, **2009**.
[25] E. Simon, P. Papoulias, P. Andrews. Gas-phase fragmentation characteristics of benzyl-aminated lysyl-containing tryptic peptides. *J. Am. Soc. Mass Spectrom.* **2010**, *21*, 1624.
[26] H. M. Fales, H. A. Lloyd, G. W. A. Milne. Chemical ionization mass spectrometry of complex molecules. II. Alkaloids. *J. Am. Chem. Soc.* **1970**, *92*, 1590.
[27] P. Longevialle, G. W. A. Milne, H. M. Fales. Chemical ionization mass spectrometry of complex molecules. XI. stereochemical and conformational effects in the isobutane chemical ionization mass spectra of some steroidal amino alcohols. *J. Am. Chem. Soc.* **1973**, *95*, 6666.

[28] O. Kanie, Y. Kanie, S. Daikoku, Y. Shioiri, A. Kurimoto, S. Mutsuga, S. Goto, Y. Ito, K. Suzuki. Multi-stage mass spectrometric information obtained by deconvolution of energy-resolved spectra acquired by triple-quadrupole mass spectrometry. *Rapid Commun. Mass Spectrom.* **2011**, *25*, 1617.

Supporting information

Additional supporting information may be found in the online version of this article at the publisher's web site.